Effect of Steric Hindrance on the Dynamics of Charge Recombination within Geminate Ion Pairs

Vauthey, Eric

How to cite

VAUTHEY, Eric. Effect of Steric Hindrance on the Dynamics of Charge Recombination within Geminate Ion Pairs. In: The journal of physical chemistry. A, 2000, vol. 104, n° 9, p. 1804–1810. doi: 10.1021/jp993522d

This publication URL: https://archive-ouverte.unige.ch/unige:3662
Publication DOI: 10.1021/jp993522d

ARTICLES

Effect of Steric Hindrance on the Dynamics of Charge Recombination within Geminate Ion Pairs

Eric Vauthey*

Institut de Chimie-Physique de l'Université de Fribourg, Pérolles, CH-1700 Fribourg, Switzerland

Received: October 1, 1999; In Final Form: December 9, 1999

The dynamics of charge recombination within geminate ion pairs formed by electron transfer (ET) quenching of excited aromatic hydrocarbons by aliphatic and aromatic amines was investigated using picosecond transient grating spectroscopy. With aliphatic donors, the rate constant of back ET, k_{BET}, shows a substantial decrease with increasing steric encumbrance around the N atom. No correlation between k_{BET} and the exergonicity of the process was observed. This effect is ascribed to a decrease of the electronic coupling matrix element, V, which is affected by both the distance between the N atom of the donor and the aromatic plane of the acceptor and by the delocalization of the hole upon increasing the bulkiness of the alkyl substituents. With aromatic amines, k_{BET} is substantially slower than with the unhindered amines. This is also explained in terms of a smaller value of V because of charge delocalization.

Introduction

Compared with intramolecular electron transfer (ET) reactions, a major difficulty related to the study of intermolecular ET in liquids is the knowledge of the geometry at which ET takes place. Recent investigations have shown that this ET geometry depends on the exergonicity of the reaction, ΔG_{ET}: weakly exergonic ET takes place at contact distance, whereas more exergonic ET apparently can occur at larger intermolecular distances.[1−5] Moreover, even in polar solvents, fluorescence quenching reactions with a small ΔG_{ET} value do not result in the direct formation of a geminate ion pair (GIP), but rather in the generation of an exciplex, which can subsequently dissociate into free ions.[6−9] It was shown that the rate constant of exciplex dissociation was correlated with ΔG_{ET}, the dissociation being faster with increasing exergonicity.[10] This was explained by an increase of the charge-transfer character of the exciplex and by a corresponding decrease of the activation energy for dissociation into free ions. Very recently, Kochi and co-workers showed that the ET geometry also strongly depends on the steric encumbrance of the ET partners[11]: ET quenching of quinones in the triplet state by unhindered alkylbenzenes results in the formation of a strongly coupled encounter complex before ET. In this case, the free energy dependence of the ET rate constant correlates poorly with the Marcus theory. On the other hand, quenching with sterically hindered alkylbenzenes does not involve a complex before ET. The corresponding ET rate constants are substantially slower than with unhindered donors and can be discussed in terms of the Marcus theory.

If steric hindrance has such a strong effect on the ET quenching, the dynamics of charge recombination (CR) can also be expected to be influenced substantially. Such an effect could not be observed with the acceptor/donor (A/D) pairs used by Kochi and co-workers.[11] Indeed, as the excited precursor is in the triplet state, the resulting GIP is also formed in a triplet state and back electron transfer (BET) within such a pair is spin forbidden. Consequently, BET is much slower than separation into free ions, and the free ion yield is high.

The influence of steric crowding on the free ion yield has been investigated by Gould and Farid using dicyano- and tetracyanoanthracene as electron acceptors and alkylbenzenes as donors.[12] For A/D pairs with similar free energies for BET, ΔG_{BET}, the separation efficiency was larger by a factor 2 to 3 with hindered than with unhindered donors. The free ion yield, Φ_{ion}, is defined as follows:

$$\Phi_{ion} = \Phi_q \cdot \Phi_{sep} = \Phi_q \cdot \frac{k_{sep}}{k_{BET} + k_{sep}} \qquad (1)$$

where Φ_q is the quenching efficiency, Φ_{sep} is the separation efficiency, k_{BET} is the rate constant of BET within the GIP, and k_{sep} is the rate constant of separation of the GIP into free ions.

From eq 1, it is immediately clear that the knowledge of Φ_{sep} alone does not allow the value of both k_{BET} and k_{sep} to be recovered. Consequently, Gould and Farid could not unambiguously ascribe the effect of steric hindrance observed on Φ_{sep} to either k_{BET} or k_{sep}.[12]

In this article, we present our investigation on the effect of steric hindrance on the dynamics of CR within GIPs generated by ET quenching of 9-cyanophenanthrene (CNP) and perylene (Pe) in the lowest excited singlet state by tertiary amines with various steric crowding (see Chart 1). Amines have been chosen for their good electron donor properties, for their availability with different degrees of steric crowding, and also for their good solubility in acetonitrile. Indeed, to be able to resolve the

* E-mail: eric.vauthey@unifr.ch

10.1021/jp993522d CCC: $19.00
Published on Web 02/10/2000

CHART 1

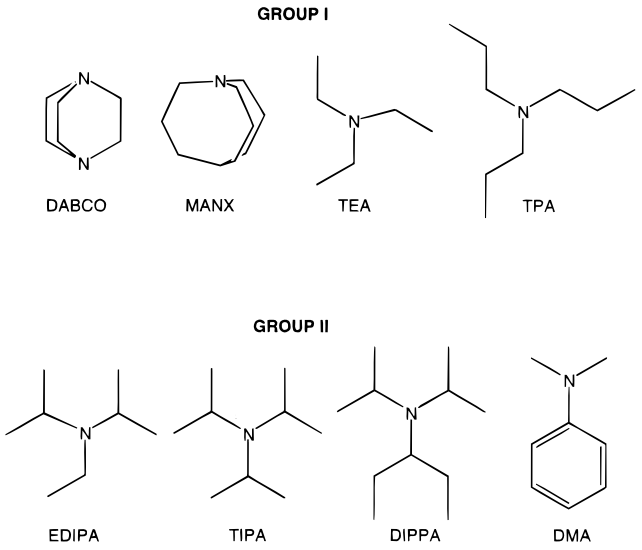

dynamics of fast CR, ET quenching must be even faster and thus high quencher concentrations are required.

The time dependence of GIP population was monitored using the transient grating (TG) spectroscopy.[13] This technique was preferred to transient absorption because of its much superior sensitivity. These data, together with the knowledge of free ion yields, allow both k_{BET} and k_{sep} to be determined and thus the effect of steric encumbrance on both processes to be investigated.

Experimental Section

Apparatus. The picosecond TG setup has been described in detail elsewhere.[13,14] The third harmonic output at 355 nm of an active/passive mode-locked Nd:YAG laser (Continuum PY61−10) was split in two parts, which were recombined, both spatially and temporally, on the sample with an angle of incidence of 0.2°. The duration of the pulse was about 25 ps, and the pump energy on the sample was about 500 μJ. The remaining laser output at 1064 nm was sent along a variable optical delay line before being focused into a 25-cm-long cell filled with a 70:30 (v/v) D_2O/H_2O mixture for continuum generation. The resulting white light pulses (450−760 nm) were spatially filtered and focused onto the sample to a spot of about 2-mm diameter with an angle of incidence of 0.25°. The diffracted signal was passed through a cutoff filter (Schott GG400) to eliminate scattered pump light and imaged onto the entrance slit of an imaging spectrograph (Oriel Multispec 257) equipped with a 1024 × 256 pixels water-cooled CCD camera (Oriel Instaspec IV). At each position of the delay line, the TG spectrum was averaged over 20 shots. For each measurement, the delay line was scanned 10 times. Each measurement was repeated three times.

The free ion yields have been determined using photoconductivity.[15] The photocurrent cell has been described in detail elsewhere.[16] The system benzophenone with 0.02 M 1,2-diazabicyclo[2,2,2]octane in acetonitrile, which has a free ion yield of unity, was used as a standard.[17]

Samples. Triethylamine (TEA), *N*,*N*-dimethylaniline (DMA), *N*-ethyldisopropylamine (EDIPA), tripropylamine (TPA), triisopropylamine (TIPA), and *N*,*N*-diisopropylpentan-3-amine (DIPPA) were dried and distilled under inert atmosphere.[18] 1-Azabicyclo[3.3.3]undecane (Manxine, MANX) was synthesized according to the literature.[19] Benzophenone (Aldrich Gold Label) and 1,2-diazabicyclo[2.2.2]-octane (DABCO) were sublimed, whereas CNP and Pe where recrystallized. Acetonitrile (ACN, UV grade) was used without further purification. Unless specified, all products were from Fluka. For TG experiments, the absorbance of the sample solutions at 355 nm was approximately 0.15 over 1 mm, the cell thickness. The donor concentration was 0.5 M except for DIPPA, in which it was 0.35 M. To avoid degradation, the samples were flowed continuously. For photoconductivity measurements, the sample absorbance at 355 nm was approximately 0.5 over 1 cm.

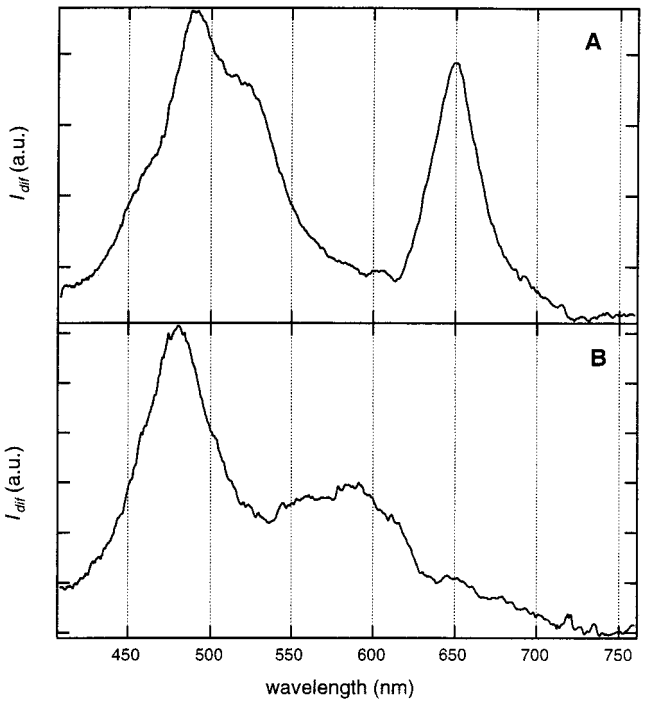

Figure 1. TG spectra measured 700 ps after excitation at 355 nm of solutions of CNP (A) and CNP and 0.35 M DIPPA (B) in ACN.

Results

Figure 1A shows the TG spectrum measured with a solution of CNP in ACN, 700 ps after excitation at 355 nm, whereas Figure 1B shows the TG spectrum measured at the same time delay with a solution of CNP and 0.35 M DIPPA in ACN. The nature of a TG spectrum has been discussed in detail elsewhere.[13,20] The diffracted intensity, I_{dif}, is proportional to the square of the photoinduced absorbance and refractive index changes. Consequently, the TG spectrum is equal to the sum of the squares of the transient dispersion spectrum and of the transient absorption spectrum. Practically, the TG spectrum is very similar to the corresponding transient absorption spectrum. The TG spectrum shown in Figure 1A corresponds to CNP in the S_1 state, which has a lifetime of 24 ns,[21] and contains a band at 490 nm with a shoulder at approximately 520 nm and a narrower band at 650 nm. The TG spectrum measured with DIPPA consists of a band at 475 nm with a pronounced shoulder at approximately 580 nm. This spectrum does not exhibit any band at 650 nm, indicating that ^{1}CNP* has been totally quenched. The spectrum in Figure 1B is mainly due to the radical anion of CNP, the absorption coefficient of the radical cation of most aliphatic amines being very small.

TG spectra very similar to that shown in Figure 1B have also been obtained using DMA, EDIPA, and TIPA as quenchers. However, the lifetime of the $CNP^{\bullet-}$ band varied strongly from one donor to another. Figure 2 shows the time profiles of the

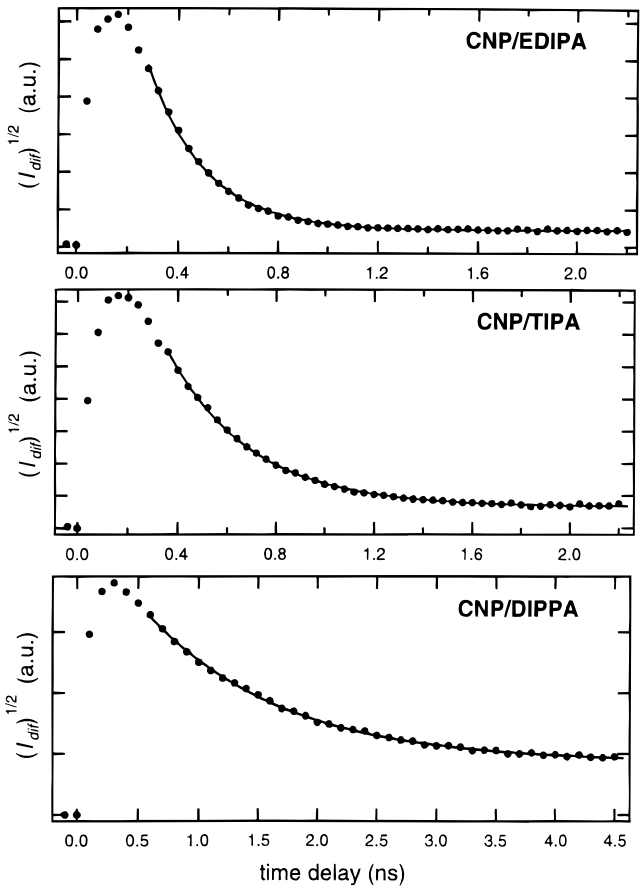

Figure 2. Time profiles of the square root of the diffracted intensity at 475 nm after excitation at 355 nm of solutions of CNP with various donors in ACN and best single-exponential fits (solid lines).

square root of the diffracted intensity at 475 nm measured with EDIPA, TIPA, and DIPPA. The square root of I_{dif} is proportional to the concentration of the transient species. These time profiles can be very well fitted with a single exponential function decaying with a rate constant k_{GIP} to a constant positive intensity, which is larger than the intensity before excitation. The monoexponential component is due to the decay of $CNP^{\bullet-}$ within the GIP by both CR to the neutral ground state and separation to free ions. The remaining intensity originates from the free $CNP^{\bullet-}$, which decay by homogeneous recombination in the microsecond time scale. Apart from a very few exceptions, the absorption spectra, hence the TG spectra of an ion within a GIP and of a free solvated ion, are identical. These two species can only be differentiated through their different time dependence: short lifetime and first-order kinetics for the GIP and long lifetime and second-order kinetics for the free ions. The values of k_{GIP} are listed in Table 1.

No $CNP^{\bullet-}$ band could be observed with TEA, DABCO, and TPA as electron donors. The TG spectra contain the ^{1}CNP* bands only, which decay in less than 100 ps, with a rate constant k_{S_1}. This effect can be explained by the fact that CR is faster than ET quenching, even at the high quencher concentration used. Because the GIP decays faster than it is formed, its contribution to the TG spectrum is much smaller than that of the precursor, ^{1}CNP*. For these two donors, only a lower limit of $k_{GIP} = k_{s_1}$ can thus be determined (see Table 1).

Figure 3A and 3B show TG spectra measured with Pe alone and with 0.5 M TIPA, 700 ps after excitation at 355 nm. The first spectrum exhibits the intense 695 nm band of ^{1}Pe* ($\epsilon = 7.5 \cdot 10^4$ M^{-1} cm^{-1}),[22] whereas the second spectrum shows the

TABLE 1: Measured Rate Constants of GIP Population Decay, k_{GIP}, and Free Ion Yields, Φ_{ion}, and Calculated Rate Constants of BET, k_{BET}, and of Separation, k_{sep}

A/D	ΔG_{ET} (eV)[a]	k_{GIP} (ns^{-1})	Φ_{ion}	k_{BET} (ns^{-1})	k_{sep} (ns^{-1})
CNP/TEA	−0.66	>16.3[b]	0.02	>16.0	>0.3
CNP/DMA	−0.84	0.77	0.46	0.42	0.35
CNP/DABCO	−0.87	>15.3[b]	0.02	>15.0	>0.3
CNP/EDIPA	−0.90	4.7	0.04	4.5	0.2
CNP/TPA	−0.92	>8.2[b]	0.02	>8.0	>0.2
CNP/TIPA	−1.11	3.0	0.06	2.82	0.18
CNP/DIPPA	−1.19	0.87	0.19	0.70	0.17
Pe/TEA	−0.29	>10.6[c]	0.06	>10	>0.6
Pe/DMA	−0.47	0.75	0.67	0.25	0.50
Pe/DABCO	−0.50	>50[c]	0.01	>50	>0.5
Pe/EDIPA	−0.53	1.84	0.14	1.58	0.26
Pe/TPA	−0.55	>10[c]	0.05	>9.5	>0.5
Pe/MANX	−0.74	>10[c]	0.05	>9.5	>0.5
Pe/TIPA	−0.74	1.51	0.22	1.18	0.33
Pe/DIPPA	−0.82	0.88	0.25	0.66	0.22

[a] CNP: $E_{red} = -1.88$ V vs SCE; $E(S_1) = 3.42$ eV.[44] Pe: $E_{red} = -1.66$ V vs SCE[45]; $E(S_1) = 2.83$ eV.[46] [b] $k_{GIP} > k_{S_1}$ [c] $k_{GIP} > 5\ k_{S_1}$

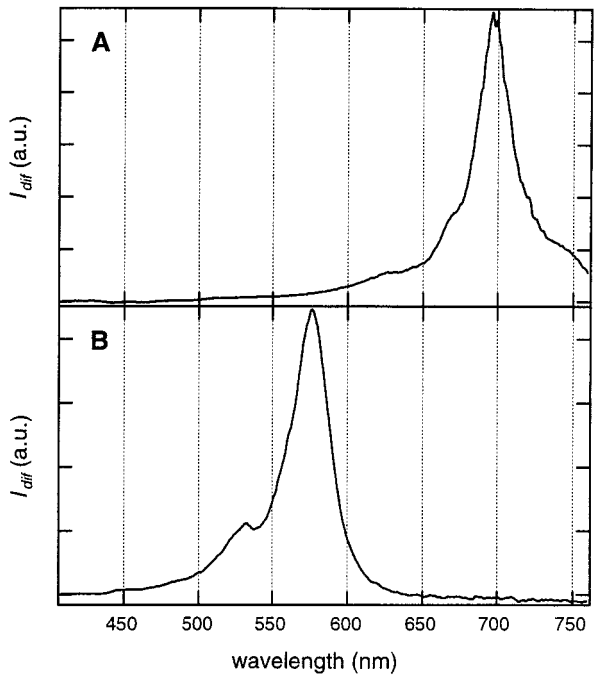

Figure 3. TG spectra measured 700 ps after excitation at 355 nm of solutions of Pe (A) and Pe and 0.5 M TIPA (B) in ACN.

575 nm band of $Pe^{\bullet-}$ ($\epsilon = 5.10^4$ M^{-1} s^{-1}).[23,24] The time profiles of the square root of the TG intensity at 575 nm, measured with several donors, are shown in Figure 4. These decays can be analyzed as those measured with CNP, and the corresponding k_{GIP} values are also listed in Table 1. In TEA, DABCO, TPA, and MANX, the $Pe^{\bullet-}$ band could not be detected, indicating that the lifetime of the GIP is shorter than that of the excited precursor. Considering the large extinction coefficient of $Pe^{\bullet-}$ at 575 nm, where ^{1}Pe* does not absorb, and the sensitivity of the experimental setup, the lifetime of the GIP must be at least five times shorter than that of ^{1}Pe* (see Table 1).

For CNP, it is safer to take k_{S_1} as a lower limit for k_{GIP}, because the TG bands of both ^{1}CNP* and $CNP^{\bullet-}$ partially overlap (see Figure 1).

The free ion yields were measured at two different donor concentrations: at that used in the TG measurements and at half this concentration. In both cases, the quenching efficiency, Φ_q, was unity and thus the separation efficiency, Φ_{sep}, was

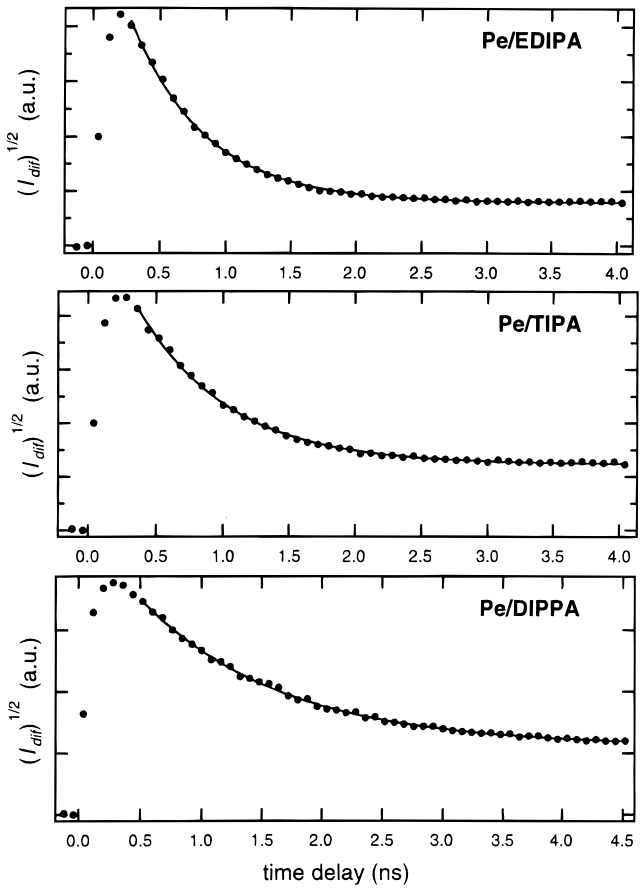

Figure 4. Time profiles of the square root of the diffracted intensity at 575 nm after excitation at 355 nm of solution of Pe with various donors in ACN and best single-exponential fits (solid lines).

identical to the free ion yield (see eq 1). For a given A/D pair, Φ_{ion} was the same at both concentrations (see Table 1).

Discussion

Equation 1 is based on the assumption that only one type of GIP is produced upon ET quenching. As shown by several authors, bimolecular ET reactions may involve two types of GIPs: the so-called contact ion pair (CIP) and the solvent separated or loose ion pair (LIP).[25−29] CIPs are formed mainly when directly exciting the charge-transfer band of the ground-state complex. The CIP can be converted further into a LIP, which can subsequently dissociate into free ions. When the forward ET occurs via diffusional quenching, CIPs are formed only if the reaction is weakly exergonic, $\Delta G_{ET} > -0.4$ eV. The CIP is characterized by its fluorescence even in polar solvents. More exergonic reactions seem to generate the LIP directly. In this case, eq 1 can be used to extract both k_{BET} and k_{sep} from k_{GIP} and Φ_{sep}, as $k_{GIP} = k_{BET} + k_{sep}$.

The ΔG_{ET} values for the A/D pairs investigated here are listed in Table 1. They were calculated using the following equation[30]:

$$\Delta G_{ET} = E_{ox}(D) - E_{red}(A) - E(S_1) \qquad (2)$$

where $E_{ox}(D)$ and $E_{red}(A)$ are the oxidation and reduction potentials of D and A, respectively and $E(S_1)$ is the energy of the excited precursor. In this equation, the correction term has been neglected, because it is generally accepted to be close to zero in polar solvents.

The oxidation potential of most aliphatic amines is unknown because these compounds often show irreversible oxidation waves. On the other hand, their adiabatic ionization potential, *aIP*, can be determined accurately. Jacques and co-workers have established the following correlation between E_{ox} and *aIP* for a series of aliphatic amines[31]:

$$E_{ox} = 0.83\ aIP - 5.34 \qquad (3)$$

where E_{ox} is in *V* vs SCE and *aIP* in eV. This relationship has been used to calculate the oxidation potential of the aliphatic amines from the *aIP* values listed in Table 2.

TABLE 2: Adiabatic Ionization Potentials, *aIP*, Molecular Volumes, V_m, Differences Between the Vertical and Adiabatic Ionization Potentials, ΔIP, Shortest Distances Between the N Atom of the Aliphatic Amines and the Aromatic Plane of the Acceptor, *d*, and Electrostatic Stabilization Energies, E_{es}

D	*aIP* (eV)	V_m (Å^3)	ΔIP (eV)	*d* (Å)	E_{es} (eV)
TEA	7.5[a,d]	126	0.55	3.8	−0.94
DABCO	7.24[b]	116	0.28	3.0	−1.21
EDIPA	7.2[a]	160	0.50	4.3	−0.83
TPA	7.18[c,d]	177	0.76	3.9	−0.91
MANX	6.95[b]	167	0.18	3.3	−1.10
TIPA	6.95[a]	177	0.25	4.7	−0.77
DIPPA	6.85[a]	211	0.35	5.0	−0.72

[a] Ref 47. [b] Ref 48. [c] Ref 49. [d] Ref 31.

Table 1 shows that, with the exception of Pe/TEA, the ET quenching for all A/D pairs is more exergonic than −0.45 eV. Consequently, these reactions should involve only one type of GIP and thus eq 1 can be used to extract k_{BET} and k_{sep} from k_{GIP}. The quenching of ^{1}Pe* by TEA might involve the formation of a CIP, although no exciplex emission could be observed even with intense laser excitation.

For all pairs studied, no absorption band indicating the formation of a ground-state complex was detected. Moreover, the ratio of the steady-state fluorescence intensity without and with quencher was identical to the ratio of the excited state lifetime, $k_{s_1}^{-1}$, without and with quencher. This indicates that the quenching is essentially dynamic and rules out the direct formation of CIP through excitation of a charge-transfer band.

The values of k_{BET} and k_{sep}, obtained using eq 1 with $k_{GIP} = k_{BET} + k_{sep}$, are listed in Table 1, whereas the free energy dependence of k_{BET} is plotted in Figure 5. The free energy for BET has been calculated as $\Delta G_{BET} = -E(S_1) - \Delta G_{ET}$. For pairs with small ion yield, the k_{sep} values should only be considered because estimates because the absolute error on Φ_{ion} is about 0.01.

The BET processes within the GIPs studied here are all highly exergonic, ΔG_{BET} lying between −3 and −2 eV. According to the Marcus theory, these BET reactions should lie in the inverted region, i.e. k_{BET} should decrease with increasing exergonicity.[32] Figure 5 shows no clear correlation between k_{BET} and ΔG_{BET}. However, the A/D pairs can be clearly separated into two groups according to their k_{BET} values: group I containing those pairs with a k_{BET} larger or equal to 10^{10} s^{-1} and group II comprising those with a k_{BET} inferior to $5 \cdot 10^9$ s^{-1}. Donors belonging to group I are TEA, DABCO, TPA, and MANX, whereas the aromatic amine DMA, as well as the aliphatic amines EDIPA, TIPA, and DIPPA belong to group II (see Chart 1).

Considering the aliphatic amines only, it is clear that the donors of the two groups can be distinguished by the different steric crowding around the nitrogen atom, from which the transferred electron has been removed. For DABCO, the N atom is accessible enough to allow van der Waals contact with CNP and Pe. For TEA, TPA, and MANX, the steric crowding is slightly larger than with DABCO, but remains small. This is

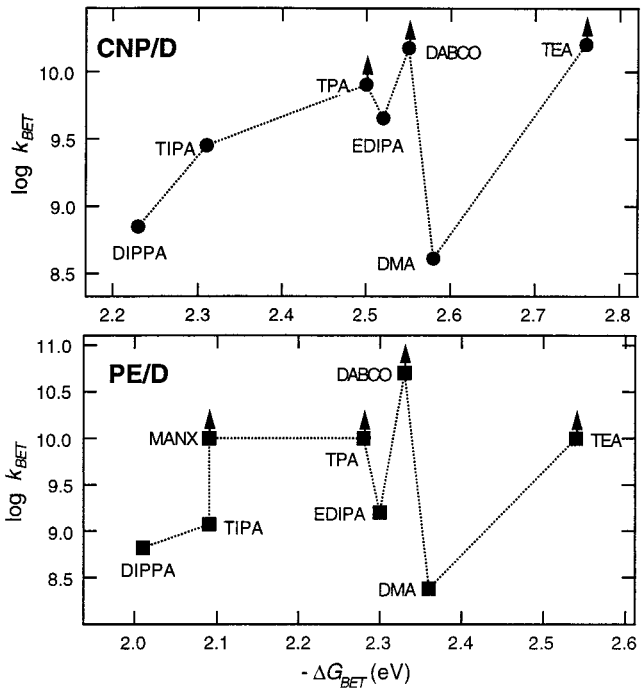

Figure 5. Free energy dependence of the BET rate constant within CNP/D and Pe/D pairs.

no longer the case with the aliphatic amines of group II. Indeed, the steric encumbrance around the N atom increases continuously from EDIPA to TIPA and to DIPPA. Table 1, shows that this increase in bulkiness is accompanied by a parallel decrease of k_{BET} with relative ratios of 6.4:4:1 for CNP and 2.4:1.8:1 for Pe. The influence of exergonicity cannot be invoked to account for this decrease. Indeed, the oxidation potential of these amines decreases from EDIPA to DIPPA and thus the exergonicity for BET increases with the steric crowding of D. As these BET take place in the inverted region, k_{BET} should increase in the order EDIPA, TIPA, and DIPPA, contrarily to the observation. This demonstrates that exergonicity is not a determining parameter for the variation of k_{BET} within these GIPs.

According to ET theories,[32,33] the other important parameters controlling the ET rate constant are the solvent and intramolecular reorganization energies, λ_s and λ_i, respectively, the average frequency of the vibrational modes coupled to ET, ν, and the electronic coupling matrix element, V.

According to the expression for λ_s derived from the dielectric continuum theory, the solvent reorganization energy depends on the molecular radii of A and D, r_A and r_D, and on their center to center distance, r_{AD}. The radius, r_D, increases with steric encumbrance and, assuming that BET takes place at contact distance, r_{AD} increases as well. The molecular volumes of the aliphatic amines, V_m, calculated using the Van de Waals increments method[34] are listed in Table 2. Apart from TPA, the amines of group I are noticeably less voluminous than those belonging to group II. Consequently, λ_s can be expected to be substantially larger for TEA and DABCO than for the other aliphatic amines, and to decrease continuously in the order EDIPA, TIPA, TPA, and DIPPA. For ET taking place in the inverted region, larger λ_s implies smaller activation energy, hence faster ET, in partial agreement with our observation. However, if λ_s were really the determining factor, TPA should belong to group II, i.e. BET within A/TPA pairs should be slower.

The internal reorganization energy, λ_i, associated with the electron donors can be estimated from the difference between the vertical and the adiabatic ionization potentials of the amines, ΔIP (see Table 2).[35] As expected, the ΔIP value of floppy amines such as TEA and TPA is larger than that of rigid amines such as MANX and DABCO, but there is no correlation between ΔIP and the steric crowding. Thus, λ_i seems not to be responsible for the variation of k_{BET} observed here. The same is certainly true for, ν, the average frequency of the vibrational modes coupled to ET. Because all these donors are aliphatic amines, similar vibrational modes must be involved, hence ν should not vary substantially from one aliphatic amine to another.

The electronic coupling matrix element V is an important parameter of ET theory, because the ET rate constant is proportional to V^2. This parameter is related to the overlap integral of acceptor and donor wave functions and its magnitude depends on two main factors. The first one is the distance between the reaction partners, the variation of V with distance usually being expressed as[32]:

$$V(d) = V_0 \exp\left(-\frac{\beta(d - d_0)}{2}\right) \qquad (4)$$

where, V_0 is the V value at contact distance, d_0, and β is a constant, which determines the rate of falloff of V with distance, d. For intermolecular ET in rigid glasses, β has been measured to be of the order of 1.0 to 1.2 $Å^{-1}$.[36,37]

The closest possible distances between the N atom of the aliphatic amines studied here and the aromatic plane of A are listed in Table 2. The structures of the molecules have been determined using AM1 calculations. This procedure has predicted accurate geometries of tertiary amines.[38] The closest van der Waals distance has been estimated by visually approaching the space-filling model of both molecules using a commercial software.[39] Of course, this procedure only gives approximate distances, but the trend shown in Table 2 is certainly significant. As expected, the shortest possible distance occurs with DABCO, where direct van der Waals contact between the N atom and the acceptor is possible. The largest distance is with DIPPA, the most encumbered amine. These data show that d is not directly correlated with the molecular volume; TPA and TIPA have the same volume but a different d value, with the N atom being obviously more hindered in TIPA.

Figure 6 shows that the distance dependence of the natural logarithm of k_{BET} for CNP/D and Pe/D pairs with the aliphatic amines is almost linear. The slope obtained from linear regression corresponds to the coefficient β, and amounts to 2 for CNP/D (without DABCO) and 2.1 for Pe/D, using also the lower limit values for TEA, DABCO, MANX, and TPA. These β values are larger than those reported for intramolecular ET in glasses. Moreover, β can be expected to be even larger, because the decrease of k_{BET} with distance should be partially counter-balanced by the parallel decrease of BET exergonicity with increasing steric hindrance, hence with distance. The distances used here have been estimated for the neutral molecules, while BET takes place between ions. As mentioned above, some variation of the geometry upon ionization can be expected for the floppier amines, such as TEA and TPA, as reflected by the ΔIP values. For these two amines, the distance d can be expected to be slightly larger for the ions than for the neutrals, as the three N−C bonds become coplanar in the cation. On the other hand, these bonds are almost already coplanar in the more sterically encumbered amines.[38] Consequently, these variations should not substantially change the trend shown in Figure 6.

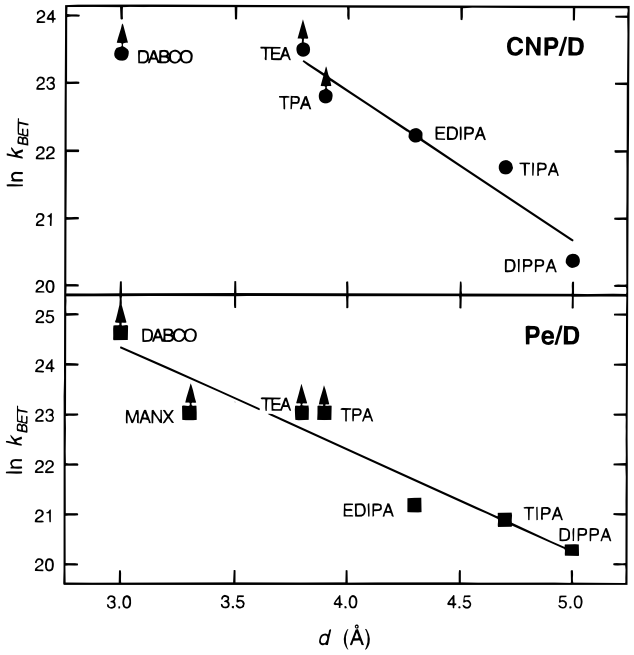

Figure 6. Distance dependence of the BET rate constant within CNP/D and Pe/D pairs.

The second factor influencing the magnitude of V is related to the localization of the charges. If these charges are spread out over a large number of atoms, the wave functions involved in the BET are more diffuse than if the charges are concentrated on a single atom, and consequently V is smaller. This effect has been invoked by Gould et al. to explain the higher ion yields measured with naphthalene derivatives than with benzene derivatives as electron donors.[43] For the α-branched aliphatic amines, the charge delocalization increases with the size of the alkyl substituents. Thus, the hole density on the N atom decreases continuously from TEA to DIPPA, although the spin remains localized on N. This increasing hole dilution should lead to a corresponding decrease of the contribution of the p orbital at the N atom to BET and to a parallel decrease of V. The stabilization of the hole through delocalization is reflected by a decrease of the vertical ionization potential of the amines upon addition of alkyl substituents ($aIP + \Delta IP$ in Table 2). Consequently, steric crowding and charge delocalization are strongly entangled. The increase of distance between the aromatic plane of A and the N atom of D, which results in a decrease of the overlap between the π system of A and the p orbital at the N atom, is accompanied by a decrease of the hole density on N. For this reason, the large β value obtained above, by neglecting the effect of charge dilution, is certainly overestimated.

Turning now to the aromatic amine, Table 1 shows that CR within the A/DMA pairs is even slower than with DIPPA, the most hindered amine. In this case as well, the magnitude of V must be substantially smaller than with DABCO or TEA. However, this decrease can only be due to the delocalization of the positive charge, which is very strong because of the presence of the aromatic ring.

A last parameter that has not been considered so far is the electrostatic interaction energy between both ions, E_{es}. A large stabilization energy would make BET less exergonic. The analytical expressions for this energy are based on the dielectric continuum model and their validity for determining E_{es} for the ion pairs discussed here is highly questionable.[30,41,42] Nevertheless, the expression predicting the largest stabilization energy will be considered. This model has been proposed by Suppan and treats the molecules as two infinite plane capacitors.[41] At contact distance, the electrostatic stabilization energy amounts to $E_{es} = -e^2/(8\pi\epsilon_0 n_m^2 d)$, n_m being the refractive index of A and D. The resulting E_{es} values calculated with $n_m^2 = 2$ are listed in Table 2. As expected, this energy becomes smaller as steric hindrance increases. However, this effect is too small, even by assuming that the hole is localized on the N atom, to change substantially the free energy dependence of k_{BET} shown in Figure 5. Indeed, for the pairs containing EDIPA, TIPA, and DIPPA, k_{BET} is still diminishing with decreasing exergonicity.

Finally, Table 1 shows that k_{sep} varies between $2{\cdot}10^8$ s^{-1} to more than $5{\cdot}10^8$ s^{-1}. Moreover, k_{sep} seems to be smaller with the sterically crowded amines (EDIPA, TIPA, and DIPPA) than with TEA and DABCO; the case of TPA is less clear. However, there seems to be a better correlation between k_{sep} and the molecular volume, V_m, which is reasonable because this process is diffusive. It is nevertheless difficult to draw definitive conclusions because half of these values are lower limits. Moreover, for the CNP/D pairs, these differences are not very pronounced and must be considered with caution, because the free ion yields are very small. However, these results confirm that the indirect determination of k_{BET} from the free ion yield and with the assumption that k_{sep} is constant for different GIPs can lead to erroneous results.

Conclusion

We have reported the first direct measurement of the effect of steric hindrance on the dynamic of CR within GIPs. These results clearly show that CR becomes slower as the bulkiness of the electron donor increases. However, this effect cannot be ascribed to pure steric effects only. The presence of bulky substituents on the N atom does not only affect the distance between A and the N atom of D but also the hole density at this atom, both effects resulting in a decrease of the electronic coupling matrix element V. In the forward ET process, the electron is transferred from an orbital localized on the N atom in all aliphatic amines. Consequently, a decrease of V upon increasing steric encumbrance should originate purely from a distance effect.

Acknowledgment. I wish to thank Prof. Thomas Bally for stimulating discussions. This work was supported by the Fonds national suisse de la recherche scientifique through project 2000-055388.98. Financial support from the Fonds de la recherche and the Conseil de l'Université de Fribourg is also acknowledged.

References and Notes

(1) Kikuchi, K.; Niwa, T.; Takahashi, Y.; Ikeda, H.; Miyashi, T. *J. Phys. Chem.* **1993**, *97*, 5070.

(2) Scully, A. D.; Takeda, T.; Okamoto, M.; Hirayama, S. *Chem. Phys. Lett.* **1994**, *228*, 32.

(3) Murata, S.; Nishimura, M.; Matsuzaki, S. Y.; Tachiya, M. *Chem. Phys. Lett.* **1994**, *200*, 219.

(4) Jacques, P.; Allonas, X. *Chem. Phys. Lett.* **1995**, *233*, 533.

(5) Matsuda, N.; Kakitani, T.; Denda, T.; Mataga, N. *Chem. Phys.* **1995**, *190*, 83.

(6) Werner, H. J.; Staerk, H.; Weller, A. *J. Chem. Phys.* **1978**, *68*, 2419.

(7) Kikuchi, K.; Niwa, T.; Takahashi, Y.; Ikeda, H.; Miyashi, T.; Hoshi, M. *Chem. Phys. Lett.* **1990**, *173*, 421.

(8) Gould, I. R.; Farid, S. *J. Phys. Chem.* **1992**, *96*, 7635.

(9) Kuzmin, M. G.; Sadovskii, N. A.; Weinstein, J.; Kutsenok, O. *Proc. Indian Acad. Sci., Chem. Sci.* **1993**, *105*, 637.

(10) Vauthey, E.; Högemann, C.; Allonas, X. *J. Phys. Chem. A* **1998**, *102*, 7362.

(11) Hubig, S. M.; Rathore, R.; Kochi, J. K. *J. Am. Chem. Soc.* **1999**, *121*, 617.
(12) Gould, I. R.; Farid, S. *J. Phys. Chem.* **1993**, *97*, 13067.
(13) Högemann, C.; Pauchard, M.; Vauthey, E. *Rev. Sci. Instrum.* **1996**, *67*, 3449.
(14) Vauthey, E.; Henseler, A. *J. Phys. Chem.* **1995**, *99*, 8652.
(15) Vauthey, E.; Pilloud, D.; Haselbach, E.; Suppan, P.; Jacques, P. *Chem. Phys. Lett.* **1993**, *215*, 264.
(16) von Raumer, M.; Suppan, P.; Jacques, P. J. *Photochem. Photobiol. A* **1997**, *105*, 21.
(17) Henseler, A.; Vauthey, E. J. *Photochem. Photobiol. A* **1995**, *91*, 7.
(18) Perrin, D. D.; Armarego, W. L. F.; Perrin, D. R. *Purification of Laboratory Chemicals*; Pergamon Press: Oxford, 1980.
(19) Coll, J. C.; Crist, D. R.; Barrio, M. C. G.; Leonard, N. J. *J. Am. Chem. Soc.* **1972**, *94*, 7092.
(20) Högemann, C.; Vauthey, E. *Isr. J. Chem.* **1998**, *38*, 181.
(21) Pilloud, D. Ph.D. Thesis, University of Fribourg, 1993.
(22) Mataga, N.; Asahi, T.; Kanda, Y.; Okada, T.; Kakitani, T. *Chem. Phys.* **1988**, *127*, 249.
(23) Shida, T. *Electronic Absorption Spectra of Radical Ions*; Elsevier: Amsterdam, 1988; Vol. Physical Sciences data 34.
(24) Cornelisse, J.; Konuk, R.; McGlynn, S. P. *J. Chem. Phys.* **1985**, *82*, 3929.
(25) Weller, A. *Pure Appl. Chem.* **1982**, *54*, 1885.
(26) Masnovi, J. M.; Kochi, J. K. *J. Am. Chem. Soc.* **1985**, *107*, 7880.
(27) Asahi, T.; Mataga, N. *J. Phys. Chem.* **1989**, *93*, 6575.
(28) Gould, I. R.; Young, R. H.; Moody, R. E.; Farid, S. *J. Phys. Chem.* **1991**, *95*, 2068.
(29) Peters, K. S.; Lee, J. *J. Phys. Chem.* **1992**, *96*, 8941.
(30) Rehm, D.; Weller, A. *Isr. J. Chem.* **1970**, *8*, 259.
(31) Jacques, P.; Burget, D.; Allonas, X. *New J. Chem.* **1996**, *20*, 933.
(32) Marcus, R. A.; Sutin, N. *Biochim. Biophys. Acta* **1985**, *811*, 265.
(33) Barbara, P. F.; Meyer, T. J.; Ratner, M. A. *J. Phys. Chem.* **1996**, *100*, 13148.
(34) Edward, J. T. *J. Chem. Educ.* **1970**, *4*, 261.
(35) Nelsen, S. In *Advances in Electron-Transfer Chemistry 3*; Mariano, P. S., Ed.; JAI Press Inc.: Greenwich, 1993; Vol. 3, p 167.
(36) Miller, J. R.; Beitz, J. V.; Huddleston, R. K. *J. Am. Chem. Soc.* **1984**, *106*, 5057.
(37) Miller, J. R.; Beitz, J. V. *J. Chem. Phys.* **1981**, *74*, 6746.
(38) Bock, H.; Göbel, I.; Havlas, Z.; Liedle, S.; Oberhammer, H. *Angew. Chem.* **1991**, *103*, 193.
(39) *Chem3D/Plus*; Cambridge Scientific Computing, Inc.: Cambridge.
(40) Ratner, M. A.; Jortner, J. In *Molecular Electronics*; Ratner, M. A., Jortner, J., Eds.; Blackwell Science, Inc.: Oxford, 1997; p 5.
(41) Suppan, P. *J. Chem. Soc. Faraday Trans. 1* **1986**, *82*, 509.
(42) Tachiya, M. *Chem. Phys. Lett.* **1994**, *230*, 491.
(43) Gould, I. R.; Ege, D.; Moser, J. E.; Farid, S. *J. Am. Chem. Soc.* **1990**, *112*, 4290.
(44) Mattes, S. L.; Farid, S., Eds. *Organic Photochemistry*; Marcel Dekker: New York, 1983; Vol. 6.
(45) Parker, V. D. *J. Am. Chem. Soc.* **1976**, *98*, 98.
(46) Parker, C. A. *Photoluminescence of Solutions*; Elsevier: Amsterdam, 1968.
(47) von Raumer, M.; Suppan, P.; Haselbach, E. *Helv. Chim. Acta* **1997**, *80*, 719.
(48) Alder, R. W.; Arrowsmith, R. J.; Casson, A.; Sessions, R. B.; Heilbronner, E.; Kovac, B.; Huber, H.; Taageperea, M. *J. Am. Chem. Soc.* **1981**, *103*, 6137.
(49) Lias, S. G.; Bartmess, J. E.; Holmes, J. F.; Levin, R. D.; Mallard, W. G. *J. Phys. Chem. Ref. Data* **1988**, *Suppl. 1*, 17.